Convective Diffusion and Adsorption in a Swarm of Spheroidal Particles

F. A. Coutelieris, V. N. Burganos, and A. C. Payatakes
Dept. of Chemical Engineering, University of Patras, and Institute of Chemical Engineering and High Temperature Chemical Processes, GR 26500 Patras, Greece

The problem of mass transfer from a Newtonian fluid to a swarm of spheroidal adsorbers under creeping flow conditions is considered using the spheroid-in-cell model to represent the swarm. The flow field within the fluid envelope for the Kuwabara type of boundary conditions is obtained from the analytical solution of Dassios et al. (1994). The complete convective diffusion equation is used to describe mass transport within the envelope so that moderate and strong diffusional terms can be taken into account. A new set of boundary conditions is used that respects mass flux and concentration continuity across the outer surface of the cell and maximizes the applicability of the spheroid-in-cell model in the convection-to-diffusion transition regime. The resulting elliptic problem in two dimensions is solved numerically. Results for the upstream and downstream concentration profiles reveal that tangential diffusion is very significant and should not be neglected for moderate and low Peclet number values. Also, the classical Levich-type of formulation, which is theoretically valid for very weak diffusional terms only, can in practice be modified to predict with fair accuracy the overall Sherwood number and the adsorption efficiency of prolate and oblate spheroids-in-cell even in moderate Peclet number cases.

Introduction

Fluid flow and mass transport through swarms of adsorbing stationary particles are commonly encountered processes that bear considerable importance in a large number of industrial and scientific applications, such as depth filtration of rural and waste water, and noncatalytic fluid-solid reactions. Modeling of the fundamental processes associated with these applications, such as flow and transport in the vicinity of single adsorbers or in particle packings, is a very old task and has been the subject of numerous investigations within a variety of scientific disciplines. In most practical cases it can be safely assumed that the fluid properties (dynamic viscosity and density) are independent of the concentration of the solute. This assumption makes it possible to uncouple the flow problem from the mass-transport problem.

The modeling of flow in the vicinity of isolated particles or in particle swarms has been considerably facilitated by the observation that, in many practical applications, the particles of the swarm are sufficiently small and the flow sufficiently slow for the creeping flow assumption to be justified. However, even for Newtonian fluids, exact analytical solutions for the problem of creeping flow through a swarm of particles are available only for the case of *regular* arrangements of uniform *spherical* particles.

The "particle-in-cell" concept has contributed significantly toward the solution of several flow problems in particle swarms. It has led to formulations that model the flow field in a particle swarm as the flow field in the region between a single solid particle and a surrounding fluid envelope. The relative dimensions of the solid particle and the fluid envelope are adjusted so that the porosity of the configuration equals the actual porosity of the particle swarm. Moreover, the flow formulation, which involves the flow equation and a set of the boundary conditions on the inner and outer surfaces of the cell, is intended to describe the actual flow in the actual swarm. Happel (1958) and Kuwabara (1959) presented two independently devised "sphere-in-cell" models to address the flow problem in packings of spheres. Two major differences between these two models can be identified: Happel's model assumes that the outer fluid surface is stationary, whereas the solid sphere moves at a constant velocity, and

that the shear stress on the outer fluid surface vanishes everywhere. Kuwabara's model, on the other hand, assumes a radial velocity distribution on the outer fluid envelope corresponding to a uniform approach velocity (the solid sphere being stationary), and that the vorticity on the outer fluid surface (rather than the shear stress) vanishes everywhere. Despite these fundamental differences, the two models have been proved to yield very similar flow fields over a wide range of porosity values (Tien, 1989). Happel (1958) and Kuwabara (1959) have also proposed cylinder-in-cell models (using formulations that were quite analogous to those used in their own sphere-in-cell models) that consider particles of cylindrical, instead of spherical, shape. These models are suitable for modeling flow through fibrous mats and arrays of parallel fibers.

Neale and Nader (1974) proposed an important improvement over the aforementioned models. They considered that the basic spherical cell is embedded in an unbounded, continuous, homogeneous, and isotropic permeable medium of the same porosity and permeability as those of the particle swarm. The flow in the permeable medium is described by Brinkman's (1947) equation. A similar employment of Brinkman's equation in cell models is encountered in the work by Prasad et al. (1990), which replaces the solid sphere of the sphere-in-cell model with a solid sphere surrounded by a spherical shell of homogeneous and isotropic porous material. This model combines features of both sphere-in-cell models developed by Happel and Kuwabara (the composite sphere with the porous shell is stationary, but the shear stress on the outer surface of the envelope is assumed to be zero) and uses Brinkman's equation to describe the fluid flow through the porous shell. The model is based on the work of Masliyah et al. (1987) whose "solid-sphere-with-porous-shell" is embedded in an unbounded fluid instead of the fluid envelope of Prasad et al.

In all the aforementioned models, particles were assumed to be either spherical or cylindrical. The majority of practical applications (including fluid-solid reactions, filtration through packed beds, and so on), however, involves particles or grains that are clearly nonspherical; in fact, their shape is closer to spheroidal than to spherical, the deviation typically increasing with time (cases of fluid-solid reaction with solid or gaseous product, deposition of material on the grain surface, and so on). Epstein and Masliyah (1972) solved numerically the flow field through clusters of spheroids under creeping flow conditions, whereas Ammar and Hsieh (1991) produced an analytical solution to the Stokes flow inside an oblate hemispheroidal cap. Recently, Dassios et al. (1994) proposed a complete spheroid-in-cell model, which is quite analogous to Kuwabara's model except for the change in geometry, and formulated a series expansion solution to the creeping flow equation.

All these flow-oriented models can be very useful for the study of mass-transport processes that usually accompany flow through particle swarms. A commonly used approach to model mass transport in the vicinity of spherical solid particles is the well-known Levich (1962) approximation. For very high Peclet number (Pe) values the diffusion layer has negligible thickness compared to the radius of the solid particle. Under this assumption, Levich calculated the overall Sherwood number (Sh_0) for mass transfer from an unbounded dilute solution to a moving solid-spherical particle that adsorbs the solute instantaneously, and obtained the expression $Sh_0 = 0.997\ Pe^{1/3}$. The factor 0.997 depends on the selection of the characteristic length (see also Adamczyk et al. (1983) and Abramzon and Fishbein (1987)). The Levich solution was also obtained independently by Friendlander (1961) and by Lochiel and Calderbank (1964).

Pfeffer and Happel (1964) and Pfeffer (1964) used Happel's model to solve the problem of mass transfer to a sphere in a swarm for high Pe values and obtained an expression of the form $Sh_0 = f(\gamma)Pe^{1/3}$, where $f(\gamma)$ is a simple analytic function of the solid volume fraction, γ. Tardos et al. (1976) used the Happel, Kuwabara and Neale and Nader models and obtained expressions of the form $Sh_0 = 0.997\ g(\epsilon)Pe^{1/3}$, where $g(\epsilon)$ is a model dependent function of the porosity, ϵ. These authors concluded that the Neale and Nader model gives somewhat better agreement with the experimental data than the other two models. They also derived an analytical expression for the removal (or adsorption) efficiency in the case of very high Peclet numbers ($10^4 \le Pe \le 10^7$).

Not too long ago, Coutelieris et al. (1993) solved analytically the problem of mass transfer to a swarm of adsorbing spheroidal particles using the spheroid-in-cell model and obtained expressions for the overall Sherwood number that are quite analogous to those of Tardos et al. (1976) for spheres-in-cell in the range of high Pe values under creeping flow conditions.

The Levich approximation, however, is not valid for moderate or low Pe values. The diffusional terms become significant and the thickness of the concentration layer becomes comparable to the solid-particle radius. These facts complicate considerably both the mass-transport equation and the boundary conditions of the problem. Brenner (1963) obtained an asymptotic solution for a particle of arbitrary shape when $Pe \to 0$, whereas Masliyah and Epstein (1972) have solved numerically the mass-transport equation for isolated oblate and prolate spheroidal particles for $Pe \le 70$. Sehlin (1969) obtained expressions for the overall Sherwood number for isolated spheroids and high Pe numbers of the form $Sh_0 = 0.991\ KPe^{1/3}$, with K a function of the aspect ratio. Numerical solutions for the isolated collector problem and for Happel's sphere-in-cell model for colloidal deposition in porous media have also been provided by Prieve and Ruckenstein (1974), Spielman and Friendlander (1974), and Elimelech and Song (1992). In both cases, the Levich-type boundary conditions have been employed for high and low Pe values. Song and Elimelech (1992) showed that the assumption of uniform concentration (equal to the bulk value) along the outer surface of a sphere-in-cell yields unacceptable values (larger than unity) for the removal efficiency. To amend this, they proposed a modified boundary condition on the outer surface of the fluid envelope and obtained values for the single collector removal efficiency in the correct range (0, 1) even for very small Pe values. Their approach, however, involves some not entirely satisfactory assumptions that will be discussed in detail later.

In the present work, we use the spheroid-in-cell model of Dassios et al. (1994) to solve the problem of mass transfer from a Newtonian fluid to a swarm of adsorbing solid spheroids under creeping flow conditions for high, moderate, and low Pe values. A new boundary condition is proposed for

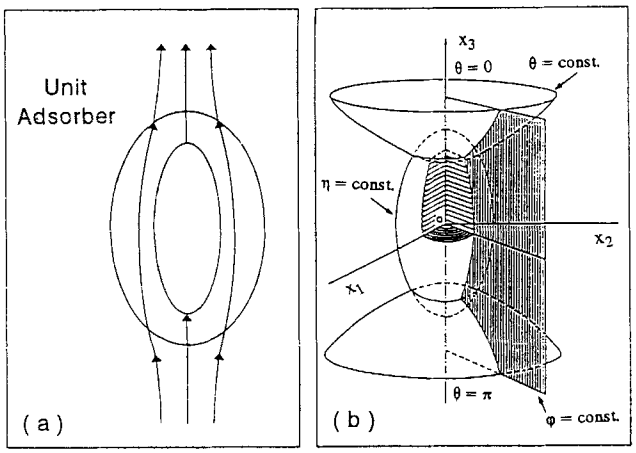

Figure 1. (a) Prolate spheroid-in-cell; (b) prolate spheroidal coordinates.

the outer fluid surface that conserves the mass flux and respects the concentration continuity across the boundary. The role of the tangential diffusion terms is examined for the first time and quantified over a broad range of *Pe* values. The thickness of the concentration layer is calculated and compared to the thickness of the fluid envelope for small, moderate, and large values of the Peclet number. Finally, the limitations of the cell models that are posed by the possible development of strong mass-transport interaction among neighboring particles in a swarm are also discussed.

Mathematical Formulation of the Problem

Prolate-in-cell case

Consider a solid stationary prolate spheroid with semiaxes $\tilde{a}_1 < \tilde{a}_3$. The semifocal distance, $\tilde{\alpha}$, is defined by $\tilde{\alpha} = \sqrt{\tilde{a}_3^2 - \tilde{a}_1^2}$, and the eccentricity by $e = \tilde{\alpha}/\tilde{a}_3$. Consider also a larger confocal prolate spheroidal surface with long semiaxis $\tilde{b}_3$ and short semiaxis $\tilde{b}_1$, surrounding the solid surface. A Newtonian fluid with dynamic viscosity $\tilde{\mu}$ and density $\tilde{\rho}$ is assumed to flow past the inner spheroid in the upward direction. This flow is caused by a uniform stream moving at a velocity of magnitude $\tilde{u}$ (at the outer boundary) in the positive z-direction (Figure 1a). The approaching fluid is a dilute solution of substance A with free stream concentration $\tilde{c}_{A,\infty}$. The solute diffuses toward the solid surface where it is adsorbed instantly. The spheroid-in-cell, which is thus obtained, is used to model mass transfer from a dilute solution to a swarm of spheroids. The dimensions of the outer spheroidal surface are determined so that the solid volume fraction of the spheroid-in-cell model is equal to that of the swarm, γ. We use $\tilde{a}_1$ as the characteristic length, $\tilde{u}$ as the characteristic velocity, and $\tilde{c}_{A,\infty}$ as the characteristic concentration for rendering all variables dimensionless. Dimensionless variables will be denoted with the same symbols as the corresponding dimensional ones, but without the tilde. Assuming now that the physical properties of the fluid ($\tilde{\mu}$ and $\tilde{\rho}$) are independent of the concentration of the solute, c_A, the hydrodynamical problem becomes uncoupled from the mass-transfer problem and can be solved separately. Dassios et al. (1994) derived an analytical solution for the creeping flow problem using a "semiseparation technique" and expressed the stream function as a series expansion. Their solution for the Kuwabara model case will be used here.

The steady-state convective diffusion equation assuming constant diffusion coefficient, $\tilde{\mathcal{D}}_{AB}$, and total concentration can be written as

$$\underline{v}\cdot\nabla c_A = Pe^{-1}\nabla^2 c_A \tag{1}$$

where $\underline{v}$ is the fluid velocity and *Pe* is the Peclet number of the process, defined by

$$Pe = \frac{\tilde{u}\tilde{a}_1}{\tilde{\mathcal{D}}_{AB}}. \tag{2}$$

Using the orthogonal prolate-spheroidal coordinates (η, θ), Figure 1b, and invoking axial symmetry, Eq. 1 becomes

$$v_\eta\frac{\partial c_A}{\partial \eta} + v_\theta\frac{\partial c_A}{\partial \theta} = \frac{Pe^{-1}}{\alpha\sqrt{\sinh^2\eta + \sin^2\theta}} \times\left[\frac{\partial^2 c_A}{\partial \eta^2} + \coth\eta\,\frac{\partial c_A}{\partial \eta} + \frac{\partial^2 c_A}{\partial \theta^2} + \cot\theta\frac{\partial c_A}{\partial \theta}\right] \tag{3}$$

where $v_\eta = v_\eta(\eta, \theta)$ and $v_\theta = v_\theta(\eta, \theta)$ are the η and θ components, respectively, of the velocity vector, θ is the polar angle, and η is constant on confocal spheroidal surfaces. On the inner spheroid $\eta = \eta_\alpha$ and on the outer boundary $\eta = \eta_\beta$. These velocity components can be obtained by differentiation of the stream function expression reported by Dassios et al. (1994). The leading term of the stream-function solution is sufficient to yield the flow field with good accuracy and is given by

$$\psi(\eta,\theta) = \frac{\alpha^2}{D}\left\{\Lambda_2 G_2(\cosh\eta) + \Lambda_3\left[\frac{5G_4(\cosh\eta_\beta)}{G_1(\cosh\eta_\beta)}G_1(\cosh\eta) + G_4(\cosh\eta)\right] + \Lambda_4 H_2(\cosh\eta)\right\}G_2(\cos\theta) \tag{4}$$

where D, Λ_2, Λ_3, Λ_4 are η and θ-dependent coefficients defined in Dassios et al. (1994) and reported in Coutelieris et al. (1993); and $G_n(x)$ and $H_n(x)$ denote the Gegenbauer polynomials of the first and second kind, respectively, of degree $-\frac{1}{2}$ and order n. The components of the dimensionless velocity, $\underline{v}$, are obtained by differentiation of ψ and use of the expressions

$$v_\eta = \frac{-1}{\alpha^2\sqrt{\sinh^2\eta + \sin^2\theta}\,\sinh\eta\sin\theta}\frac{\partial\psi}{\partial\theta} \tag{5a}$$

and

$$v_\theta = \frac{1}{\alpha^2\sqrt{\sinh^2\eta + \sin^2\theta}\,\sinh\eta\sin\theta}\frac{\partial\psi}{\partial\eta}. \tag{5b}$$

For high values of Peclet number ($Pe \geq 1{,}000$) the terms containing the first- and second-order θ-derivatives of the

concentration on the righthand side of Eq. 3 are negligible compared to the corresponding η-derivatives. Consequently, the problem is parabolic in θ and the appropriate boundary conditions are

$$c_A = 0 \quad \text{on} \quad \eta = \eta_\alpha \tag{6a}$$

$$c_A = 1 \quad \text{as} \quad \eta \to \infty \tag{6b}$$

$$c_A \text{ is finite} \quad \text{on} \quad \theta = \pi \quad (\eta \neq \eta_\alpha). \tag{6c}$$

If the curvature and tangential diffusion terms on the righthand side of Eq. 3 are neglected and boundary conditions 6a, 6b and 6c are used, a Levich-type of formulation for spheroids-in-cell obtains that solved analytically by Coutelieris et al. (1993). Below we discuss the boundary conditions just given, modify them and suggest new ones that can apply to cases with moderate and low *Pe*.

Equation 6a expresses instantaneous adsorption on the solid surface and remains valid over the entire *Pe* range; it should change only if the adsorption kinetics are modified.

For high *Pe* values condition 6b is practically equivalent to the condition

$$c_A = 1 \quad \text{on} \quad \eta = \eta_\beta \tag{6d}$$

since the thickness of the diffusion layer is much smaller than the thickness of the fluid envelope. This boundary condition, however, is not valid for low *Pe* values and, if used in Happel's sphere-in-cell model, it may yield values for the adsorption efficiency that are larger than unity. This observation led Song and Elimelech (1992) to the formulation of a modified boundary condition that is intended to remain valid when diffusion becomes significant, and that reduces to Eq. 6b for high *Pe* values. This formulation predicts adsorption (or colloidal deposition) efficiency estimates that remain smaller than unity even for very low *Pe* values. For prolate spheroids-in-cell this boundary condition can be written as

$$\upsilon_\eta(\eta_\beta^-, \theta) c_A - \frac{Pe^{-1}}{\alpha\sqrt{\sinh^2\eta + \sin^2\theta}} \frac{\partial c_A}{\partial \eta} = \upsilon_\eta(\eta_\beta^+, \theta) \quad \text{for} \quad \pi/2 \le \theta \le \pi \tag{7a}$$

and

$$\frac{\partial c_A}{\partial \eta} = 0 \quad \text{on} \quad \eta = \eta_\beta \quad \text{for} \quad 0 \le \theta < \pi/2 \tag{7b}$$

where the superscripts + and − denote the outer and the inner side of the outer boundary, respectively. Equation 7a expresses the flux continuity for substance A on the downstream half of the outer boundary, whereas Eq. 7b is obtained from 7a, assuming concentration continuity along the upstream half of the same boundary. This formulation, however, can lead under certain conditions (see below) to a significant discontinuity of the concentration across the downstream half of the outer fluid boundary ($c_A(\eta_\beta^-, \theta) \neq c_A(\eta_\beta^+, \theta)$ for $\theta > \pi/2$).

An alternative boundary condition is proposed here that is valid over a broad range of *Pe* values (including moderate and relatively low ones). It ensures continuity of the concentration across the entire outer surface and reduces to Eq. 6d for high *Pe* values. This condition can be written as

$$\frac{\partial c_A}{\partial \eta} = 0 \quad \text{on} \quad \eta = \eta_\beta \quad \text{for} \quad 0 \le \theta < \pi \tag{8a}$$

$$c_A = 1 \quad \text{at} \quad (\eta, \theta) = (\eta_\beta, \pi). \tag{8b}$$

Equation 8a expresses the condition that molecular diffusion across the outer boundary is nil, whereas tangential molecular diffusion (in addition to convective transport) may be significant. Considering Eq. 7a, it becomes evident that Eq. 8a expresses the continuity of the η-component of the molar flux across the outer boundary and ensures that the solute concentration is continuous at any point of the outer boundary. Equation 8b requires that the thickness of the diffusion layer be smaller than that of the fluid envelope at the point of the impact. This assumption is expected to be valid over a wide range of *Pe* values, and hence it is applicable to most practical cases.

The boundary condition described by Eq. 6c customarily has been used in the literature (see, for example, Levich, 1962; Adamczyk et al., 1983) in a variety of equivalent forms. Elimelech and Song (1992) removed the θ-convection term from the lefthand side of Eq. 3 along the stagnation line segment $\theta = \pi$, $\eta_\alpha \le \eta \le \eta_\beta$, and neglected the θ-diffusion terms from the righthand side of the same equation. Hence, an ordinary differential equation was obtained that was solved numerically using $c_A(\eta = \eta_\beta, \theta = \pi) = 1$ and $c_A(\eta = \eta_\alpha, \theta = \pi) = 0$. The resulting concentration profile was then used as the initial condition for a numerical integration with respect to θ. In this work, the axial symmetry condition is employed on the line of impact, which is written as

$$\frac{\partial c_A}{\partial \theta} = 0 \quad \text{on} \quad \theta = \pi, \quad \eta_\alpha \le \eta \le \eta_\beta \tag{9}$$

and implies nil θ-component of the molar flux, N_{A_θ} (Prieve and Ruckenstein, 1974; Christ and Oliver, 1990). The condition

$$c_A = 1 \quad \text{on} \quad \theta = \pi, \quad \eta_\alpha < \eta \le \eta_\beta \tag{10a}$$

$$c_A = 0 \quad \text{on} \quad \theta = \pi, \quad \eta = \eta_\alpha \tag{10b}$$

is valid only for very high *Pe* values (Levich, 1962; Pfeffer, 1964), and will be avoided here. The axial symmetry condition can also be written on the exit axis segment

$$\frac{\partial c_A}{\partial \theta} = 0 \quad \text{on} \quad \theta = 0, \quad \eta_\alpha \le \eta \le \eta_\beta. \tag{11}$$

Equation 11 is needed when the second-order tangential diffusion term ($\partial^2 c_A / \partial \theta^2$) is retained in the convective diffusion equation. A diagram of the BCs used in the full model is shown in Figure 2.

To summarize, our approach of attacking the problem is to retain all the convection and diffusion terms in the original Eq. 3, and use the boundary conditions 6a, 8a, 8b, 9 and 11. The sole assumption incorporated in our model is the exis-

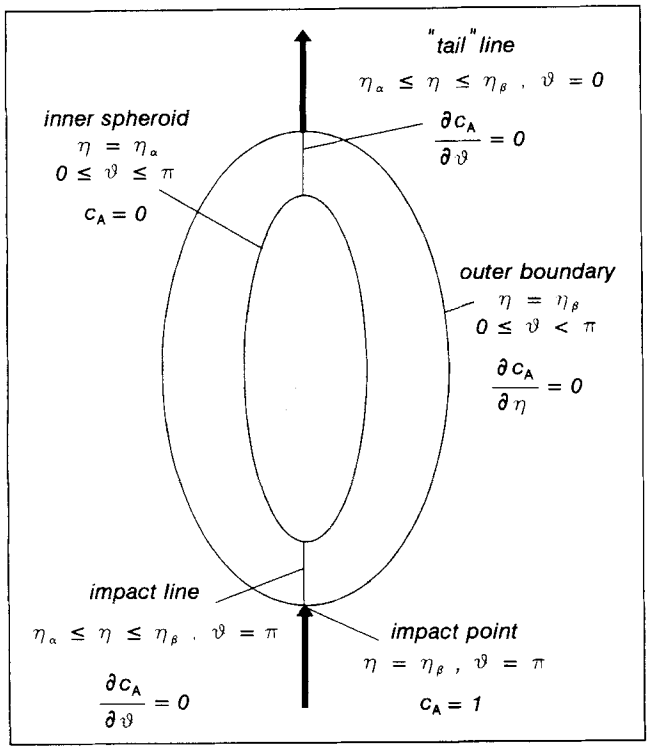

Figure 2. BCs used in the full model.

tence of at least one point within the fluid region (namely, the point of impact $(\eta, \theta) = (\eta_\beta, \pi)$), where the concentration of A has its bulk value. This assumption seems to be inevitable in view of the definition of the grain-in-cell model. For very low Pe values the predictions of this model can be viewed as normalized values with respect to the concentration of A at the point of impact (which, of course, is not equal to the bulk concentration in this case). Solution of the diffusion-limited problem in the general case of (nonregular) particle arrangements can only be accomplished through a global model that considers a sufficiently large sample of the actual swarm and solves the flow and mass-transport equations in the interparticle space.

The set of Eqs. 3, 6a, 8, 9 and 11 was discretized using finite differences on a variable mesh (finer in the impact and tail regions and coarser in the equatorial zone). Convergence of the numerical techniques was achieved using a 120×120 grid in spheroidal coordinates. In order to quantify the role of the tangential diffusion terms, we repeated our calculations, having neglected them. In this case, an initial-value, two-point boundary-value problem is obtained and Eq. 3 reduces to an ordinary differential equation on the line of impact $\theta = \pi$, $\eta_\alpha \le \eta \le \eta_\beta$ $(v_\theta = 0)$. Solution of this ode with the boundary conditions 6a and 8a provides the concentration profile along the upstream stagnation line, which then serves as initial condition for the integration of Eq. 3 (without the tangential diffusion terms) with respect to θ. Cubic spline collocation on finite η elements followed by θ-integration were used instead of finite differences to obtain fine details of the concentration profile wherever needed. For the sake of comparing our results with those obtained with the Levich approximation (negligible curvature and tangential diffusion terms, and bulk concentration value on the outer surface), as well as with the boundary condition proposed by Song and Elimelech (1992), we have repeated the calculations considering each of these cases separately. The analytical solution of Coutelieris et al. (1993) was used in the case of the Levich formulation.

Oblate-in-cell case

The oblate-in-cell case $(\tilde{a}_1 > \tilde{a}_3)$ can be treated in a similar manner using the oblate spheroidal coordinates $(\bar{\eta}, \theta)$. The convective diffusion equation becomes

$$\bar{v}_\eta \frac{\partial \bar{c}_A}{\partial \bar{\eta}} + \bar{v}_\theta \frac{\partial \bar{c}_A}{\partial \theta} = \frac{Pe^{-1}}{\bar{\alpha}\sqrt{\cosh^2 \bar{\eta} - \sin^2 \theta}} \times \left[\frac{\partial^2 \bar{c}_A}{\partial \bar{\eta}^2} + \tanh \bar{\eta} \frac{\partial \bar{c}_A}{\partial \bar{\eta}} + \frac{\partial^2 \bar{c}_A}{\partial \theta^2} + \cot \theta \frac{\partial \bar{c}_A}{\partial \theta} \right] \quad (12)$$

where $\bar{v}_\eta$ and $\bar{v}_\theta$ are the $\bar{\eta}$ and θ components of the velocity vector calculated by Dassios et al. (1994).

The expressions needed to describe the boundary conditions are identical to those in the prolate-in-cell case, except for the flux-continuity Eq. 7a in the model by Song and Elimelech (1992), which for oblate spheroids becomes

$$\bar{v}_\eta(\bar{\eta}_\beta, \theta)\bar{c}_A - \frac{Pe^{-1}}{\bar{\alpha}(\cosh^2 \bar{\eta} - \sin^2 \theta)^{1/2}} \frac{\partial \bar{c}_A}{\partial \bar{\eta}} = \bar{v}_\eta(\bar{\eta}_\beta^+, \theta) \quad \text{for} \quad \pi/2 \le \theta \le \pi. \quad (13)$$

The numerical solution of the preceding equations and the calculation of the concentration profile proceed exactly as in the case of the prolate-in-cell.

Adsorption Efficiency and Overall Sherwood Number

Prolate-in-cell case

The single adsorption efficiency of a grain-in-cell is defined as

$$\lambda_0 = \frac{\text{rate of adsorption}}{\text{rate of upstream influx}}.$$

For spheroids-in-cell we can write

$$\lambda_0 = \frac{I}{\tilde{u}\tilde{c}_{A,\infty}\pi \tilde{b}_1^2} \quad (14)$$

where

$$I = \iint_{\tilde{S}_{ps}} \left[-\tilde{N}_{A_\eta} \right]_{\eta = \eta_\alpha} d\tilde{S}_{ps}. \quad (15)$$

In Eq. 15 $[-\tilde{N}_{A_\eta}]_{\eta = \eta_\alpha}$ is the η-component of the molar flux on the collector surface. It easily can be shown that

$$\lambda_0 = \frac{2}{Peb_1^2} \int_\pi^0 \left(\frac{\partial c_A}{\partial \eta} \right)_{\eta = \eta_\alpha} \sin\theta \, d\theta. \tag{16}$$

Equation 16 also gives the removal efficiency of a unit collector in the case of diffusion and deposition of Brownian particles in prolate spheroids-in-cell under the assumption of sticking coefficient equal to unity. The value of λ_0 can be calculated numerically once the η-component of the concentration gradient on the solid surface is known. We have used a modified Newton-Cotes method with adjustable step size for the evaluation of the integral on the righthand side of Eq. 16 to cope with the nonuniform mesh employed in the finite-difference solution.

The overall Sherwood number is defined as

$$Sh_0 = \frac{\tilde{k}_0 \tilde{a}_1}{\tilde{\mathfrak{D}}_{AB}} \tag{17}$$

where $\tilde{k}_0$ is the overall mass-transfer coefficient (see, also, Coutelieris et al. (1993)) defined from

$$\tilde{k}_0 (\tilde{c}_{A,\infty} - \tilde{c}_{A,s}) \tilde{S}_{ps} = 2\pi \tilde{a}_1 \tilde{\mathfrak{D}}_{AB} \int_\pi^0 \left(\frac{\partial c_A}{\partial \eta} \right)_{\eta = \eta_\alpha} \sin\theta \, d\theta. \tag{18}$$

Note that $\tilde{k}_0$ is the coefficient of mass transfer from the free stream to the solid surface. Combining Eqs. 17 and 18 yields

$$Sh_0 = \frac{1}{\left(1 + \frac{a_3}{\alpha} \sin^{-1} e\right)} \int_\pi^0 \left(\frac{\partial c_A}{\partial \eta} \right)_{\eta = \eta_\alpha} \sin\theta \, d\theta. \tag{19}$$

Alternatively, the overall Sherwood number can be defined as the average value of the local Sherwood number over the inner spheroidal surface:

$$Sh'_0 = \frac{1}{\tilde{S}_{ps}} \iint_{\tilde{S}_{ps}} Sh(\theta) \, d\tilde{S}_{ps} = \frac{1}{\left(1 + \frac{a_3}{\alpha} \sin^{-1} e\right)} \int_\pi^0 \frac{1}{c_A(\eta_\beta, \theta)} \left(\frac{\partial c_A}{\partial \eta} \right)_{\eta = \eta_\alpha} \sin\theta \, d\theta. \tag{19'}$$

This definition uses the rate of mass transfer from the outer boundary (where the concentration is not, in general, equal to the free-stream concentration) to the inner spheroid. In the particular case of a very high *Pe* value, it turns out that $c_A(\eta_\beta, \theta) = 1$. Then Eq. 19′ reduces to Eq. 19 and the two definitions lead to identical estimates of Sh_0.

Oblate-in-cell case

The expression for the adsorption efficiency in the oblate-in-cell case is quite analogous to that in the prolate-in-cell case,

$$\bar{\lambda}_0 = \frac{2}{Pe\bar{b}_1^2} \int_\pi^0 \left(\frac{\partial \bar{c}_A}{\partial \bar{\eta}} \right)_{\bar{\eta} = \bar{\eta}_\alpha} \sin\theta \, d\theta, \tag{20}$$

whereas the overall Sherwood number based on the mass-transfer rate from the free stream to the inner spheroid is given by

$$\overline{Sh}_0 = \frac{1}{\left(1 + \frac{\bar{a}_3^2}{2\bar{\alpha}} \ln \frac{1+\bar{e}}{1-\bar{e}}\right)} \int_\pi^0 \left(\frac{\partial \bar{c}_A}{\partial \bar{\eta}} \right)_{\bar{\eta} = \bar{\eta}_\alpha} \sin\theta \, d\theta \tag{21}$$

where $\bar{e}$ $(= \bar{\alpha})$ is the eccentricity of the oblate spheroid. If the mass-transfer rate from the cell boundary to the solid surface is used, the following expression obtains:

$$\overline{Sh}'_0 = \frac{1}{\left(1 + \frac{\bar{a}_3^2}{2\bar{\alpha}} \ln \frac{1+\bar{e}}{1-\bar{e}}\right)} \int_\pi^0 \frac{1}{\bar{c}_A(\bar{\eta}_\beta, \theta)} \left(\frac{\partial \bar{c}_A}{\partial \bar{\eta}} \right)_{\bar{\eta} = \bar{\eta}_\alpha} \sin\theta \, d\theta. \tag{21'}$$

Numerical evaluation of these quantities is done using the same integration procedure as that followed in the prolate-in-cell case (see earlier).

Results and Discussion

Concentration profiles at different angular positions for a very large *Pe* value (= 10,000) are presented in Figure 3a, b for prolate and oblate spheroids-in-cell, respectively. The solid curves represent the results of the complete model, that is, of the formulation that uses the complete convective-diffusion equation with the new set of boundary conditions 6a, 8, 9 and 11. The dashed curves were obtained by application of the Levich-type formulation, which neglects the curvature and tangential diffusion terms and uses the boundary conditions 6a, b, c that assume fixed concentration (equal to the bulk value) on the outer surface (Coutelieris et al., 1993). Note the excellent agreement between the two approaches in the impact region ($\theta = \pi$) and on the equator ($\theta = \pi/2$) and their very small deviation in the exit region ($\theta = 0$). Numerical investigation of the role of the tangential diffusion and curvature terms showed that their contribution to the concentration profile was negligible as expected for this high *Pe* value. On the contrary, decreasing the *Pe* value to 1,000 (which is still large) causes a significant deviation between the two approaches at $\theta = 0$, whereas for $\theta = \pi/2$ and $\theta = \pi$ a satisfactory agreement is observed (Figure 4). It was found that the deviation obtained at this *Pe* value was due solely to the existence of the curvature term in the complete model, whereas the tangential diffusion terms proved of no importance. The error of the simplified model at $\theta = 0$ stems from the fact that adsorption and convection are competitive mechanisms of solute motion in the downstream part of the cell, rendering the diffusion process significant even for a high *Pe* value. This deviation, however, is confined to the tail region, and therefore is expected to have a very small effect on the overall adsorption efficiency (see below).

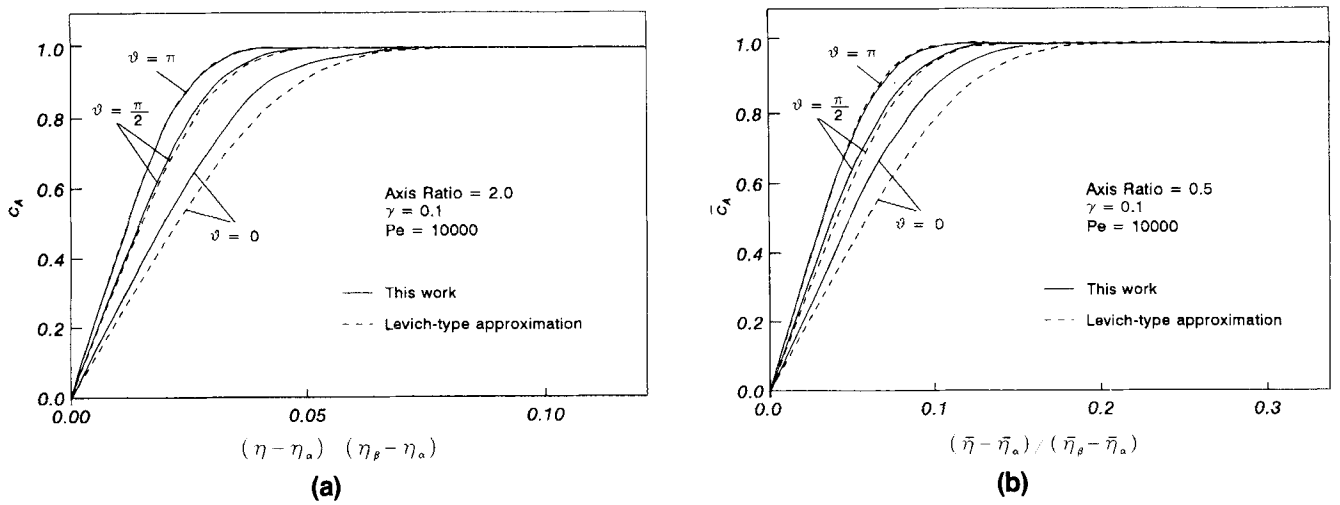

Figure 3. Concentration profiles for very high Peclet number in the vicinity of adsorbing prolate (a) and oblate (b) spheroids-in-cell at three different positions on a meridian plane.

Comparison between the numerical predictions of this work with the analytical solution based on the Levich approach and produced by Coutelieris et al. (1993) for spheroidal geometry.

Figure 5 shows the concentration profiles for a moderate Pe value ($Pe = 10$) as obtained with the formulation suggested in this work (solid curves), with a modified Levich approach that retains the curvature term but neglects tangential diffusion and uses the fixed concentration boundary conditions 6a, b, c (dashed curves), and with the Song and Elimelech-type of approximation (dotted curves). Note that in the upstream region ($\theta = \pi$) the modified Levich approach gives almost identical results to those of the Song and Elimelech approximation. Both of these approaches, however, neglect tangential diffusion and consequently overestimate the actual concentration value even in the impact region for both prolate (a) and oblate (b) geometries. This deviation becomes more pronounced downstream and becomes maximal on the exit stagnation line ($\theta = 0$).

The significance of the tangential diffusion terms for moderate Pe values can be quantified directly from Figure 6, where concentration profiles obtained with and without the employment of these terms and for the same set of boundary conditions (those of the complete model) are plotted for prolate (a) and oblate (b) spheroids-in-cell. The role of the tangential diffusion terms for moderate Pe values proves significant even in the impact region ($\theta = \pi$) and becomes progressively more pronounced as the exit region ($\theta = 0$) is approached. The tangential diffusion effect on the concentration layer is shown in Figure 7 for prolate (a) and oblate (b) spheroids-in-cell. The diffusion layer is assumed to extend here to positions where the concentration attains the value $c_A = 0.99$. For $Pe = 10$ it is seen that employment of the tangential diffusion terms in the complete model results in in-

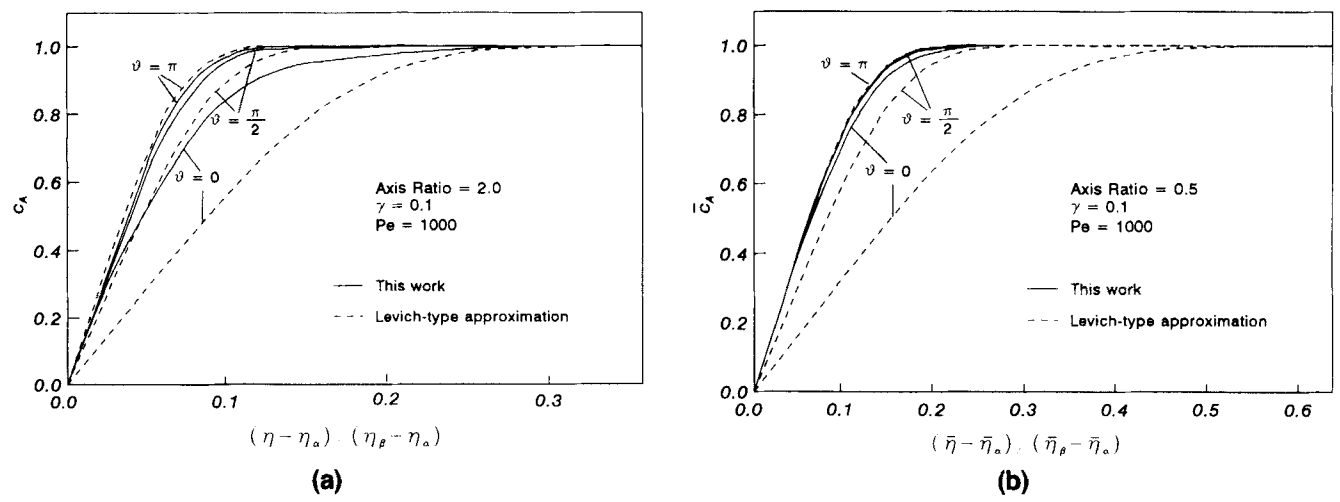

Figure 4. Concentration profiles for high Peclet number in the vicinity of adsorbing prolate (a) and oblate (b) spheroids-in-cell at three different angular positions.

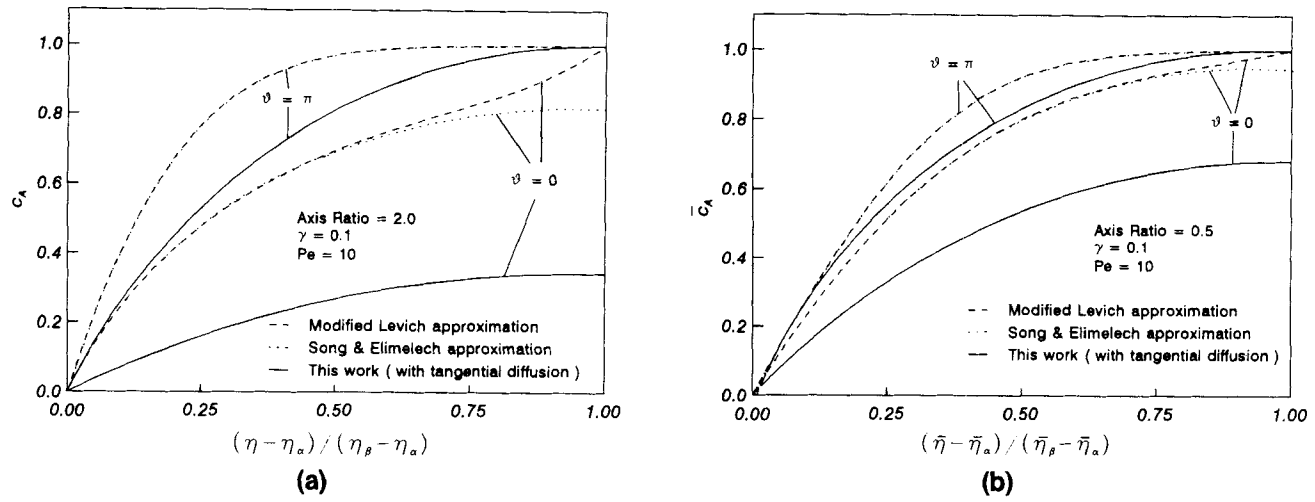

Figure 5. Concentration profiles for a moderate *Pe* value for adsorbing prolate (a) and oblate (b) spheroids-in-cell in the upstream ($\theta = \pi$) and downstream ($\theta = 0$) regions.

creased layer thickness, which becomes equal to the fluid envelope thickness at (prolate case) or near (oblate case) the equator of the cell. Omission of these terms leads to underestimation of the diffusion layer thickness, further decrease of which is observed with the Song and Elimelech formulation. Nevertheless, all three aforementioned approaches predict crossing of the outer boundary by the concentration layer. This is not the case, however, when the Levich-type of formulation is used, which forces the diffusion layer to lie entirely within the fluid envelope thanks to the employment of the $c_A = 1$ condition at the outer boundary. Note also that increasing the *Pe* value to 50 leads to convergence of all four approaches examined in this figure to the same layer profile at any angular position for both prolate and oblate geometries.

The dependence of the overall Sherwood number on the *Pe* value for prolate and oblate spheroids-in-cell is shown in Figure 8a and b, respectively. For $Pe \geq 20$ the modified Levich approach appears capable of predicting the correct Sh_0 value with sufficient accuracy, the curvature and the tangent diffusion terms being practically unimportant. For $Pe < 20$, however, these terms become significant and the three approaches mentioned in this figure predict different Sh_0 values. The modified Levich approximation yields Sh_0 values that are weakly dependent on the *Pe* value and converge to a limiting value as $Pe \to 0$. This value is a function of porosity and axis ratio only, and is given by

$$Sh_0^* = 2\alpha\left(1 + \frac{a_3^2}{\alpha}\sin^{-1}\frac{\alpha}{a_3}\right)^{-1}\left[\ln\frac{\alpha + b_3}{b_1(\alpha + a_3)}\right]^{-1} \quad (22)$$

for prolate spheroids-in-cell, and by

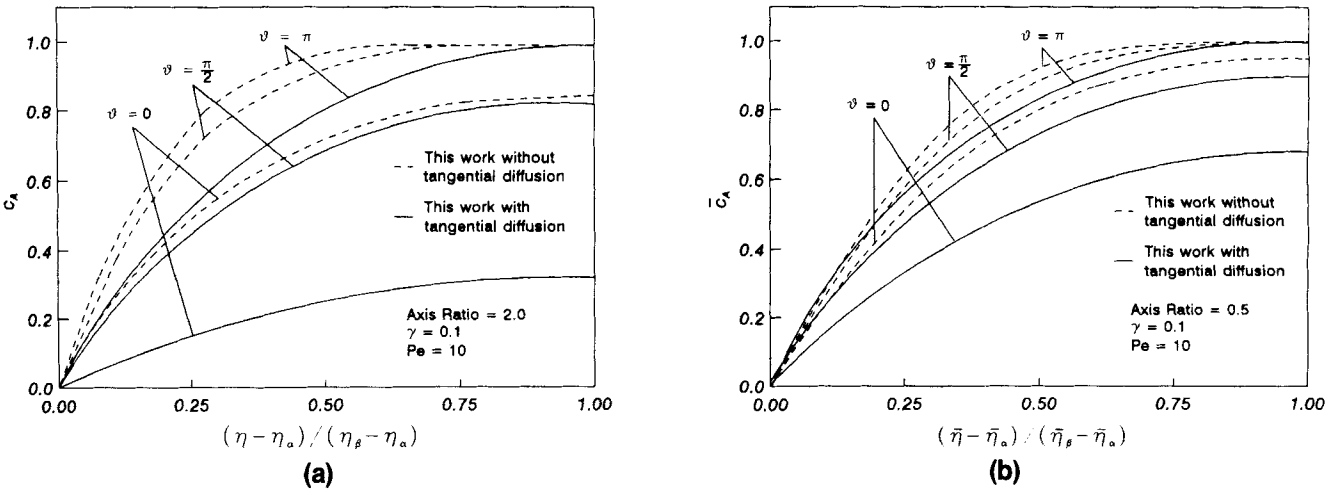

Figure 6. Concentration profiles for a moderate *Pe* value in the vicinity of an adsorbing prolate (a) and oblate (b) spheroid at three angular positions; effect of tangential diffusion.

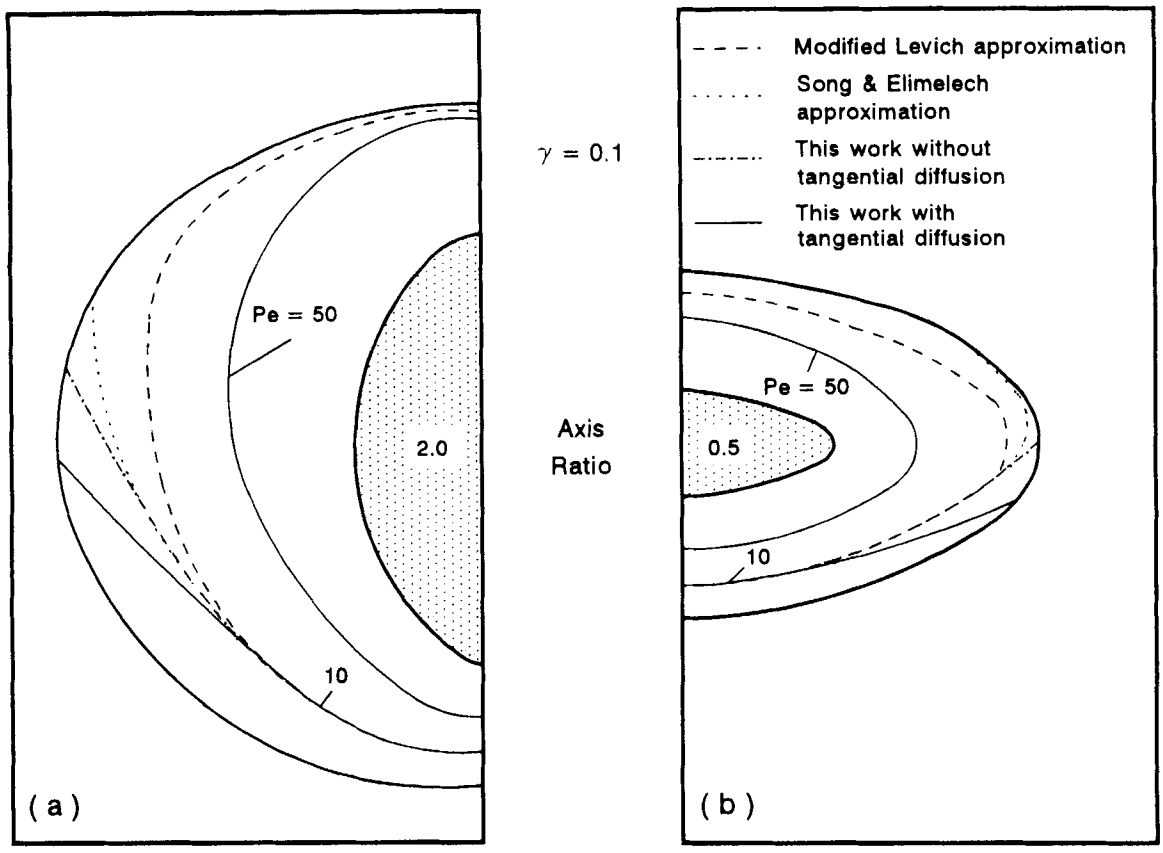

Figure 7. Profiles of the diffusion layers for prolate (a) and oblate (b) spheroids-in-cell for two *Pe* values (*Pe* = 50 and *Pe* = 10).

$$\overline{Sh}_0^* = 2\bar{\alpha}\left(1+\frac{\bar{a}_3^2}{2\bar{\alpha}}\ln\frac{1+\bar{\alpha}}{1-\bar{\alpha}}\right)^{-1} \times\left[\tan^{-1}\left(\bar{b}_3/\bar{\alpha}\right)-\tan^{-1}\left(\bar{a}_3/\bar{\alpha}\right)\right]^{-1} \quad (23)$$

for oblate spheroids-in-cell. Equations 22 and 23 result from solving the Laplace equation (retaining only the η-component of diffusion) in spheroidal coordinates using the Dirichlet conditions $c_A = 0$ on the solid surface and $c_A = 1$ on the outer surface of the fluid envelope (surfaces of constant η

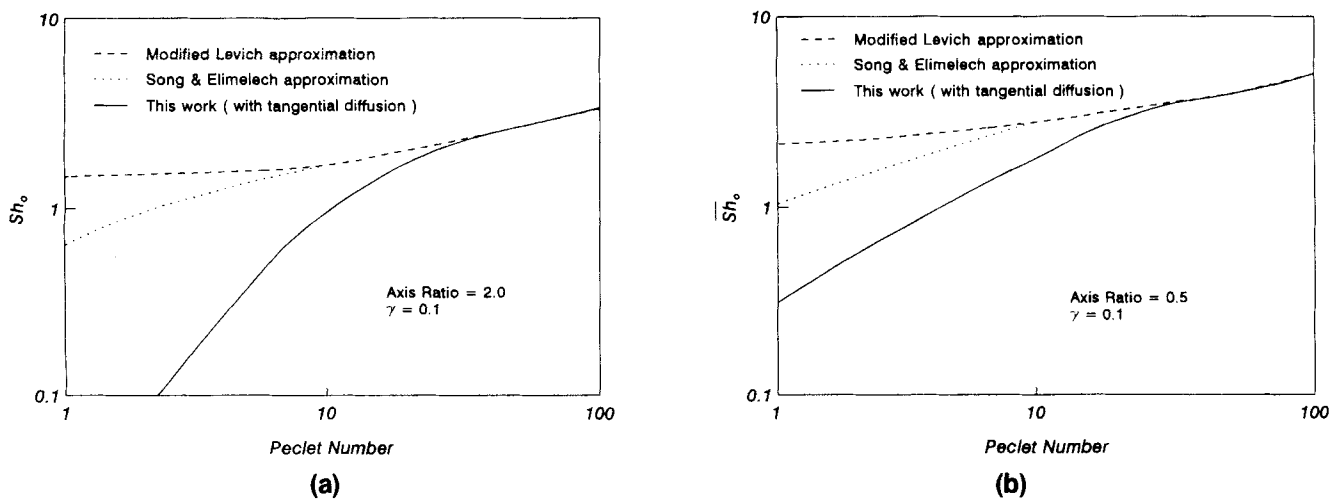

Figure 8. Dependence of the overall Sherwood number (free-stream based, Eqs. 19 and 21 on the Peclet number for prolate (a) and oblate (b) spheroids-in-cell.

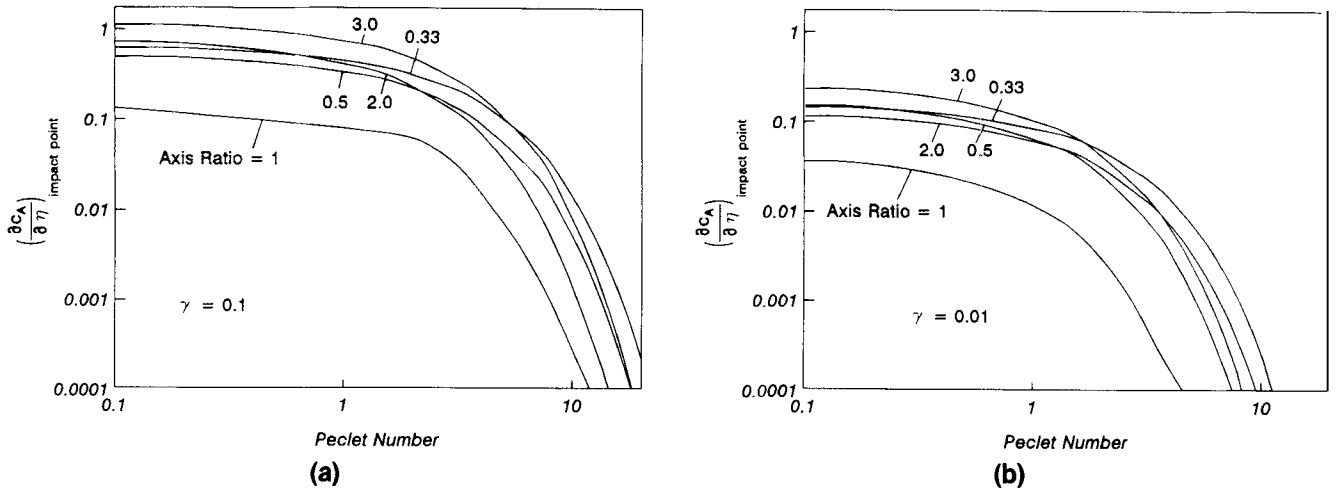

Figure 9. Test of the outer-boundary condition continuity at the impact point for various axis ratio and *Pe* values.

are surfaces of constant concentration in the pure diffusion limit, and consequently tangential diffusion is negligible). It is evident, though, that this formulation is not valid for low *Pe* values (much less for $Pe = 0$), and can only serve for the prediction of Sherwood number values in the isolated collector case, that is, for $\gamma \to 0$ ($\eta_\beta \to \infty$). The other two approaches, that is, the one proposed here and the Song and Elimelech approximation, predict Sh_0 values that are considerably lower than those obtained by the modified Levich approach and become very small as $Pe \to 0$. This is an obviously erroneous behavior and falls as a mere consequence of the limitation of the cell-model concept, which is meaningful only if interactions among neighboring cells are absent or negligibly small. Calculations with the model proposed here reveal that for $Pe < 5$ the condition $(\partial c_A/\partial\eta) = 0$ at $(\theta = \pi,\ \eta = \eta_\beta)$ is not satisfied, and hence the boundary condition posed on the surface $\eta = \eta_\beta$ becomes discontinuous at the impact point.

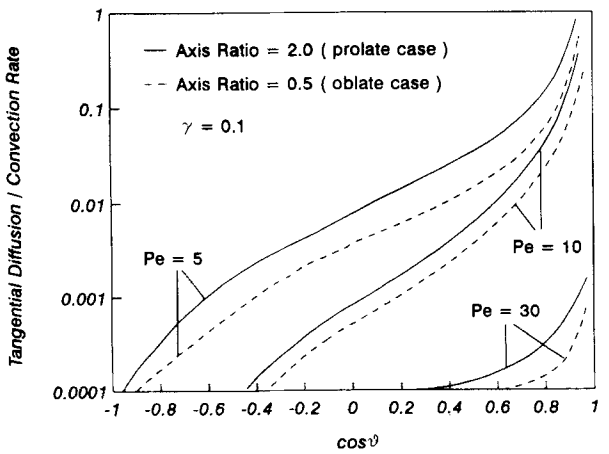

Figure 10. Ratio of the tangential components of the diffusive and convective fluxes along the outer boundary surfaces of (a) prolate and (b) oblate spheroids-in-cell for three *Pe* values.

This implication appears only in the low *Pe* value range and is due to the fact that the diffusional terms become sufficiently strong to force the concentration at the impact point (η_β, π) to be below the free-stream value. Values of $(\partial c_A/\partial\eta)$ at the impact point (η_β, π) over a broad range of *Pe* values and for several axis ratio values that cover both prolate and oblate geometries are given in Figure 9. It is seen that the critical *Pe* value below which the model is no longer valid is a rather weak function of the axis ratio, but depends strongly on the solid volume fraction of the swarm. Note that the applicability of the present formulation extends well into the transition regime. Figure 10 provides a further test of the model validity. Here, the ratio of the tangential components of the diffusive and convective fluxes on the outer boundary of prolate (a) and oblate (b) spheroids-in-cell is plotted against θ for two *Pe* values. It is seen that tangential diffusion is slow compared to convection along the cell boundary which, in combination with our boundary condition $(\partial c_A/\partial\eta)_{\eta=\eta_\beta} = 0$, shows that a slow diffusion region envelopes the cell even in the moderate and relatively low *Pe* value range and provides a further justification of our formulation.

It is very interesting to observe the fair agreement of the modified Levich approximation and the present formulation regarding the prediction of the cell-envelope-based Sherwood number (Eqs. 19′ and 21′) even in the moderate and low *Pe* value range (Figure 11a, b). This agreement is exclusively attributed to the increase of the mass-transfer coefficient in our model (thanks to its definition based on the outer concentration instead of the free-stream one) and not to improved behavior of the Levich approximation, which remains invariant under the change in the Sherwood number definition.

The dependence of the cell-envelope-based Sherwood number on the aspect ratio of the inner spheroid is presented in Figure 12 for two values of the solid volume fraction and two *Pe* values. In all cases it is noted that the Sherwood number increases with decreasing axis ratio: as the length of the axis that is normal to the approaching stream increases, mass transfer toward the solid spheroid is facilitated. For $\gamma = 0$ our results for $Pe = 1{,}000$ coincide with the results re-

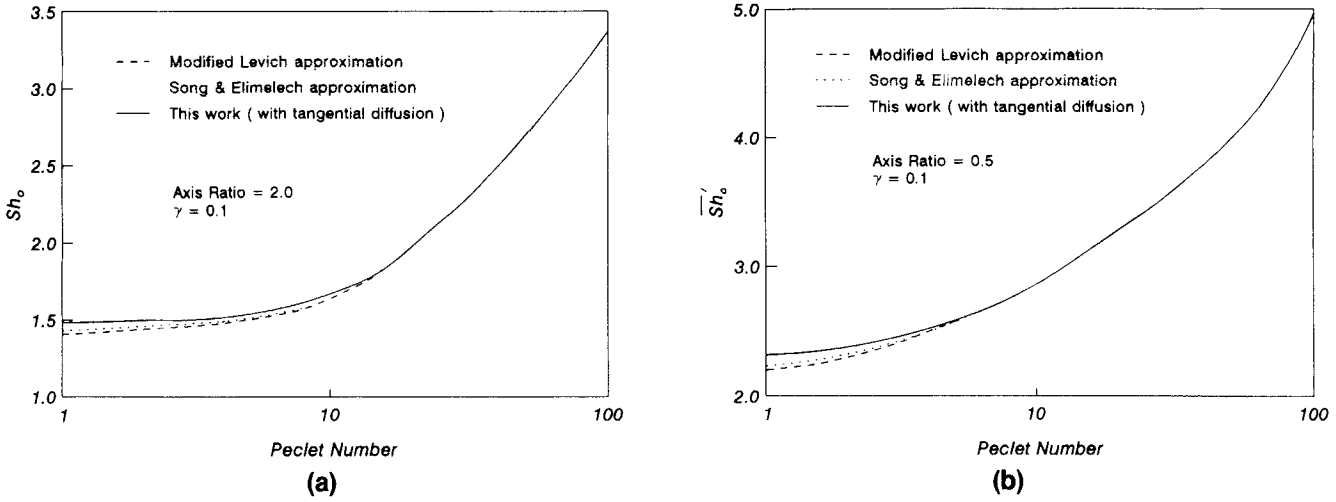

Figure 11. Dependence of the overall Sherwood number (cell-envelope based, Eqs. 19′, 21′) on the Peclet number for prolate (a) and oblate (b) spheroids-in-cell.

ported by Sehlin (1969) for isolated spheroids and high *Pe* values.

Figures 13a and 13b present adsorption efficiency results for prolate and oblate spheroids-in-cell. The modified Levich approach overestimates the adsorption efficiency for $Pe < 20$ and, if applied to *Pe* values lower than ~ 1.5, adsorption efficiency values larger than unity are obtained for both types of geometry. On the contrary, both our model and the Song and Elimelech approach predict λ_0 values, which remain lower than unity even in the low *Pe* value range.

Conclusions and Further Remarks

The problem of convective diffusion through a swarm of instantaneously adsorbing spheroidal particles is considered. The spheroid-in-cell model is used as a basis for the development of a flow and diffusion model. The fluid was assumed Newtonian, flowing under creeping conditions with approach velocity parallel to the axis of symmetry of the spheroid. The boundary conditions for the flow problem were identical to those used in Kuwabara's sphere-in-cell model (at the outer boundary, the tangential component of the fluid velocity was taken equal to the component of the approach velocity in that direction and the vorticity was assumed nil). The creeping flow problem in prolate and oblate spheroids-in-cell under the aforementioned conditions has been solved analytically by Dassios et al. (1994) who used the stream function formulation in spheroidal coordinates, devised a novel semiseparation procedure, and obtained a series-expansion solution for the stream function. The fluid velocity can be calculated in a straightforward manner at any point within the fluid envelope. The complete convective diffusion equa-

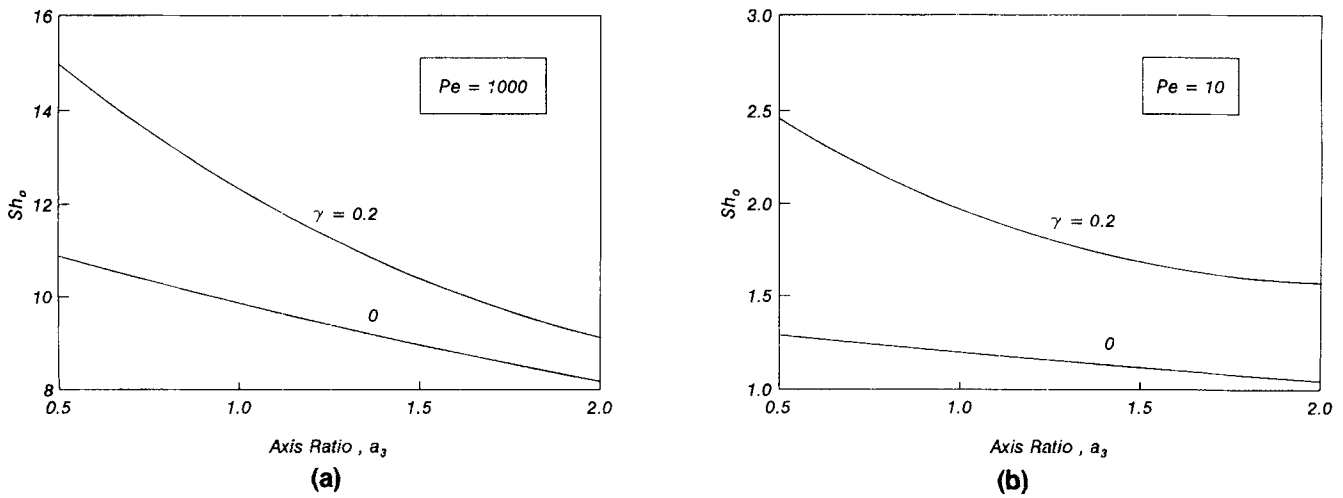

Figure 12. Dependence of the overall Sherwood number (cell-envelope based, Eqs. 19′, 21′) on the axis ratio for two values of the solid volume fraction.

(a) $Pe = 1{,}000$; (b) $Pe = 10$.

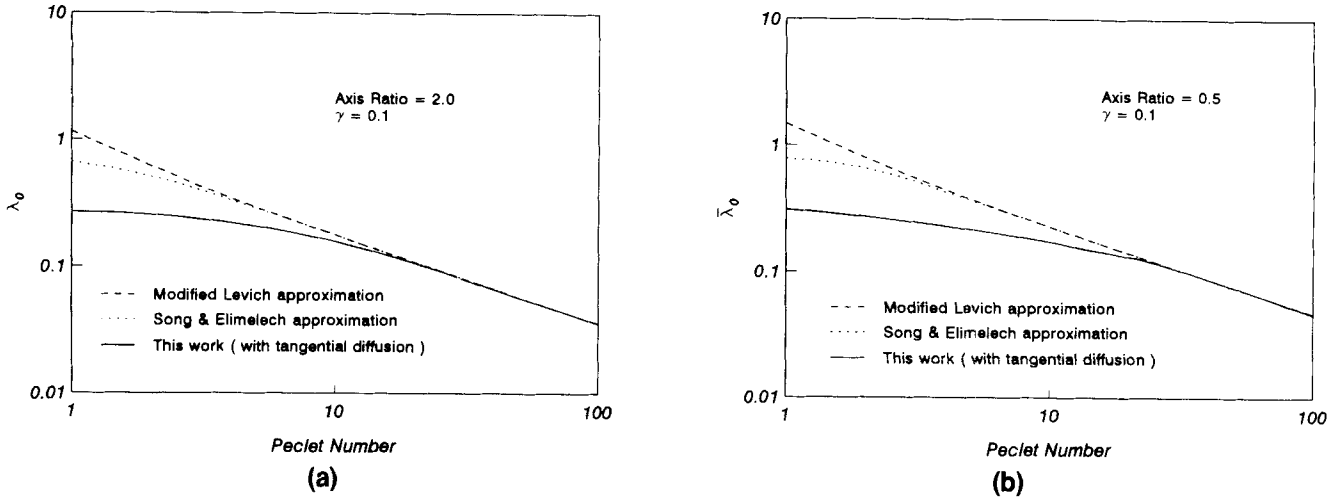

Figure 13. Dependence of the adsorption efficiency on the Peclet number for prolate (a) and oblate (b) spheroids-in-cell.

tion in spheroidal coordinates is used here to describe mass transport of a dissolved species through the envelope. In its full form this equation involves first- and second-derivative terms for the concentration and yields a two-point boundary-value problem in two dimensions (η and θ spheroidal coordinates). Flux and concentration continuity are respected by the outer boundary condition used in this work. The concentration at the point of impact (stagnation point) is used for the normalization of the interior concentration and assumed to equal the concentration of the approaching fluid at infinity. Hence, the model proposed here is not limited to high *Pe* values only and can cope with significant diffusional terms. The concentration layer is not necessarily contained within the fluid envelope (as is the case of previous simplified models) and can actually cross the outer boundary of the cell. The sole restriction that appears in this model is the requirement that the concentration layer cannot contain the entire cell. This is not a restriction posed by our formulation, however, but can be traced to the conceptual limitations of the cell model itself. The complete convective diffusion equation and the accompanying boundary conditions are discretized using a variable mesh–finite difference scheme and solved over a wide range of *Pe* values.

It was found that the assumptions of our model are valid in the moderate and high *Pe* range. The critical *Pe* value below which the model is no longer valid is a strong function of the solid-volume fraction of the cell and a weak function of the aspect ratio of the solid spheroid. For aspect ratio values between 1 and 2 this critical *Pe* value is of the order of 5. It must be emphasized that the model presented in this work makes optimal use of the cell model definition and features, and breaks down only where the cell concept is invalidated (that is, in cases of strong interaction among neighboring cells—not particles—of the swarm). Comparison of the model predictions with those of the Levich-type approximation reveals that the latter are reliable in the high *Pe* range ($Pe >$ 1,000) only. If the curvature term is retained in the convective diffusion equation, however, the Sherwood number predictions of this modified Levich formulation become of acceptable accuracy down to $Pe \approx 20$. This limiting *Pe* value decreases to $Pe \approx 1$ if the mass-transfer coefficient (needed for the Sh_0 calculation) is defined using the solute concentration drop across the fluid envelope (instead of the concentration difference from the free stream to the solid surface). The formulation suggested by Song and Elimelech (1992) for sphere-in-cell models, on the other hand, was shown to perform quite well in the prolate and oblate spheroidal geometries. Despite the considerable deviation of the concentration profiles obtained with that formulation from those yielded by our model, the overall Sherwood number was predicted with acceptable accuracy in the moderate *Pe* value range. However, the Song and Elimelech approximation neglects tangential diffusion and, consequently, cannot be applied to moderate or low *Pe* cases safely. Moreover, this approximation makes the assumption that the outer boundary concentration is continuous across only the downstream half of the boundary. This assumption can be justified only in the case of insignificant diffusion (that is, when a flowing front advances through the cell in the direction parallel to the axis of symmetry). Instead, the formulation presented here preserves the concentration and flux continuity across the cell boundaries and maximizes the range of applicability of the unit adsorber model into the regime of significant diffusional limitations. The proposed boundary conditions also have the advantage of simplicity.

Acknowledgment

This work was supported financially by the Institute of Chemical Engineering and High Temperature Chemical Processes.

Literature Cited

Abramzon, B. M., and G. A. Fishbein, "Heat and Mass Transfer with a Chemical Reaction During Motion of a Gas Bubble in a Quiescent Liquid," *J. Eng. Phys.*, **32**, 682 (1977).

Adamczyk, Z., T. Dabros, J. Czarnecki, and T. G. M. Van de Ven, "Particle Transfer to Solid Surfaces," *Adv. Colloid Interf. Sci.*, **19**, 198 (1983).

Ammar, L., and C. K. Hsieh, "Solution of the Velocity and Pressure Fields for Stokes Flow Inside an Oblate Hemispheroidal Cap," *Eur. J. Mech., B/Fluids*, **10**, 171 (1991).

Brenner, H., "Stokes Resistance of an Arbitrary Particle," *Chem. Eng. Sci.*, **18**, 109 (1963).
Brinkman, H. C., "A Calculation of the Viscous Force Exerted by a Flowing Fluid on a Dense Swarm of Particles," *Appl. Sci. Res.*, **A1**, 21 (1947).
Christ, R. W., and D. L. R. Oliver, "Nusselt Number of a Sphere in Creeping Flow," *Int. Commun. Heat Mass Transf.*, **17**, 653 (1990).
Coutelieris, F. A., V. N. Burganos, and A. C. Payatakes, "On Mass Transfer from a Newtonian Fluid to a Swarm of Adsorbing Spheroidal Particles for High Peclet Numbers," *J. Colloid Interf. Sci.*, **10**, 43 (1993).
Dassios, G., M. Hadjinicolaou, and A. C. Payatakes, "Generalized Eigenfunctions and Complete Semiseparable Solutions for Stokes Flow in Spheroidal Coordinates," *Quart. Appl. Math.*, **52**, 157 (1994).
Elimelech, M., and L. Song, "Deposition of Colloids in Porous Media—Theory and Numerical Solution," *ACS Symp. Ser.*, **491**, 26 (1992).
Epstein, N., and J. H. Masliyah, "Creeping Flow through Clusters of Spheroids and Elliptical Cylinders," *Chem. Eng. J.*, **3**, 169 (1972).
Friendlander, S. K., "A Note on Transport to Spheres in Stokes Flow," *AIChE J.*, **7**, 347 (1961).
Happel, J., "Viscous Flow in Multiparticle Systems: Slow Motion of Fluids Relative to Beds of Spherical Particles," *AIChE J.*, **4**, 197 (1958).
Happel, J., and H. Brenner, *Low Reynolds Number Hydrodynamics*, Prentice-Hall, Englewood Cliffs, NJ (1965).
Kuwabara, S., "The Forces Experienced by Randomly Distributed Parallel Circular Cylinders or Spheres in a Viscous Flow at Small Reynolds Numbers," *J. Phys. Soc. Japan*, **14**, 527 (1959).
Levich, V. G., *Physicochemical Hydrodynamics*, Prentice-Hall, Englewood Cliffs, NJ (1962).
Lochiel, A. C., and P. H. Calderbank, "Mass Transfer in the Continuous Phase around Axisymmetric Bodies of Revolution," *Chem. Eng. Sci.*, **19**, 471 (1964).
Masliyah, J. M., and N. Epstein, "Numerical Solution of Heat and Mass Transfer from Spheroids in Axisymmetric Flow," *Prog. Heat Mass Transf.*, **6**, 613 (1972).
Masliyah, J. H., G. M. Neale, K. Malysa, and T. G. M. Van de Ven, "Creeping Flow Over a Composite Sphere: Solid Core with Porous Shell," *Chem. Eng. Sci.*, **42**, 245 (1987).
Neale, G. H., and W. K. Nader, "Prediction of Transport Processes within Porous Media: Creeping Flow Relative to a Fixed Swarm of Spherical Particles," *AIChE J.*, **20**, 530 (1974).
Pfeffer, R., "Heat and Mass Transport in Multiparticle Systems," *Ind. Eng. Chem. Fund.*, **3**, 380 (1964).
Pfeffer, R., and J. Happel, "Analytical Study of Heat and Mass Transfer in Multiparticle Systems at Low Reynolds Numbers," *AIChE J.*, **10**, 605 (1964).
Prasad, D., K. A. Narayan, and R. P. Chhabra, "Creeping Fluid Flow Relative to an Assemblage of Composite Spheres," *Int. J. Eng. Sci.*, **28**, 215 (1990).
Prieve, D. C., and E. Ruckenstein, "Effect of London Forces upon the Rate of Deposition of Brownian Particles," *AIChE J.*, **20**, 1178 (1974).
Sehlin, R. S., MS Thesis, Carnegie-Mellon Univ., Pittsburgh (1969).
Song, L., and M. Elimelech, "Deposition of Brownian Particles in Porous Media: Modified Boundary Conditions for the Sphere-in-Cell Model," *J. Colloid Interf. Sci.*, **153**, 294 (1992).
Spielman, L. A., and S. K. Friendlander, "Role of the Electrical Double-layer in Particle Deposition by Convective Diffusion," *J. Colloid Interf. Sci.*, **46**, 22 (1974).
Tardos, G. I., C. Gutfinger, and N. Abuaf, "High Peclet Number Mass Transfer to a Sphere in a Fixed or Fluidized Bed," *AIChE J.*, **22**, 1147 (1976).
Tien, C., *Granular Filtration of Aerosols and Hydrosols*, Series in Chemical Engineering, Butterworths, Boston (1989).

Manuscript received Apr. 4, 1994, and revision received Aug. 3, 1994.